CrossMark

MRS Advances © 2017 Materials Research Society
DOI: 10.1557/adv.2017.171

# Temperature-dependent Optical Properties of AlN Thin Films by Spectroscopy Ellipsometry

Yao Liu[1,2], Ehsan Ghafari[2], Xiaodong Jiang[2], Yining Feng[2], Zhe Chuan Feng[1], Ian Ferguson[3] and Na Lu[2,*]
[1]Laboratory of optoelectronic materials & detection technology, Guangxi Key Laboratory for the Relativistic Astrophysics, School of Physical Science & Technology, Guangxi University, Nanning, 530004, China
[2]Lyles School of Civil Engineering, School of Materials Engineering, Birck Nanotechnology Center, Purdue University, West Lafayette, IN 47906, U.S.A.
[3]Dept. Elect. Comp. Engineering, Missouri Science and Technology, Rolla, MO 65409, U.S.A.

## ABSTRACT

In this work, temperature-dependent optical properties of a series of AlN thin films with different thickness are studied by spectroscopic ellipsometry (SE) ranging from 300 to 825K. The fitted refractive index at 300K is in good agreement with the reported by others, which confirms the high accuracy of the optical model used in this work. The degradation of the absorption properties and the decrease of the bandgap become more pronounced with temperature increases above 475K. A larger change of bandgap at elevated temperature is observed for the thinner AlN epi-layer (300nm) than the thicker ones (404nm). This can be attributed to the poor surface morphologies and crystal qualities in the thinner AlN epi-layer.

## INTRODUCTION

AlN films have become a promising candidate for a wide range of applications including high-temperature power electronics, piezoelectric sensors, ultraviolet (UV) light emitting diodes (LEDs), and UV detectors. This is due to their unique material properties such as high thermal conductivity, high thermal stability, large dielectric breakdown field, high surface velocity of acoustic wave (SAW) and ultra-wide bandgap [1-6]. To optimize its high temperature application potentials, it is important to understand the optical constants and bandgap variation of AlN with the function of temperature. Several experimental methods have been employed to study the temperature-dependent optical properties of AlN thin films in the past. For instance, Watanable *et al.* [7] evaluated the refractive index of AlN films up to temperatures of 788K by using optical interference measurements. Sohal *et al.* [8] and He *et al.* [9] reported the bandgap of AlN films on low temperature (20-450K) by using optical transmission spectroscopy. Nam *et al.* [10] utilized deep UV photoluminescence spectroscopy to evaluate the temperature-dependent bandgap energy in AlN thin films from 10 to 800K. However, PL measurement cannot investigate the thermo-optic effect. Optical constants and film thickness can be estimated with very high precision by using ellipsometry, since this technique measures relative light intensities modulated by optical elements [11]. M. Röppischer *et al.* [12] investigated the dielectric function (DF) of zinc-blende AlN determined by ellipsometry. Feneberg *et al.* [13] reported the low-temperature-dependent exciton resonances in the DF of wurtzite AlN derived by spectroscopic ellipsometry (SE) from 5 to 295K over a 2-6.4eV spectral range. Rossbach *et al.* [14] discussed the temperature dependence (10-296K) of the extraordinary and ordinary DF of wurtzite AlN



Downloaded from https://www.cambridge.org/core. Purdue University Libraries, on 03 Nov 2017 at 14:42:42, subject to the Cambridge Core terms of use, available at https://www.cambridge.org/core/terms. https://doi.org/10.1557/adv.2017.171

using ellipsometry. However, there have been no studies reported on the effect of high temperatures on the optical properties of AlN films by using ellipsometry method. In this work, the temperature (300-825K) dependent optical constants and bandgaps of AlN/sapphire thin films are studied with different thickness of epitaxial layers using a Mueller matrix ellipsometer.

## EXPERIMENT

The AlN samples were grown on c-plane (0001) sapphire substrates by metal-organic chemical vapor deposition (MOCVD) technique. A 12 nm-thick low-temperature (LT) AlN interlayer was firstly deposited on the sapphire substrate at 600$^{o}$C, then the temperature was raised to 1100$^{o}$C to grow high-temperature (HT) AlN epitaxial layer. For comparison, three samples (namely AlN-1, AlN-2, and AlN-3) with different thickness of epitaxial layers were studied in this work.

Spectroscopic ellipsometry was used as a non-destructive method to precisely evaluate optical constants, thickness of layers and surface roughness. Temperature-dependent (from 300K to 825K) ellipsometry parameters (psi and delta) of the three samples in the wavelength range (195nm-1650 nm) were measured at three incident angles of 50$^{o}$, 55$^{o}$ and 60$^{o}$, by using a dual rotating-compensator Muller matrix ellipsometer (ME-L ellipsometer) [15] equipped with a Linkam heating and freezing stage system (THMS600). Atomic force microscope (AFM) was used to characterize the surface morphology. The root mean square of the surface roughness of the three samples was found to between 14.1 to 2.3 nm for 10×10μm$^{2}$ area for different thickness of epitaxial layers, which can be used as the initial values of surface roughness for the SE fitting procedure. A four-layer model using Eometrics software was developed to describe the material structures including sapphire substrate, two AlN layers and surface roughness. One Tanguy oscillator, one Tauc-Lorentz oscillator and one Gaussian oscillator were used for the AlN layers. The surface roughness was a mixture of AlN/voids over-layer modeled by Bruggeman effective medium approximation (EMA). Based on the best-fit optical models and fitting algorithms, surface roughness, layer thickness, the dependence of refractive index and absorption coefficient of the samples with various temperatures were derived. The fitting results are in good agreement with measured results as mean squared error (MSE) is lower than 10.

## DISCUSSION

The surface roughness and thickness of AlN epitaxial layer were derived from SE fitting as listed in Table 1. Figure 1, for example, shows the fitting results of ellipsometric spectra for AlN-3 sample at 825K, and the interference oscillations below the bandgap corresponding to the transparent region of the sample. The surface roughness of AlN-1 was substantially larger than the other two samples. The reason can be attributed to the thinner layer of AlN-1, which could induce a partially relaxed structure. Figure 2 shows the refractive index ($n$) of all three samples extracted by SE fitting at 300K. It is observed that the refractive index increases with the increasing thickness of epi-layer, which is in consistent with the existing literatures [2, 16]. Figure 2 also shows the fitted refractive index from Ref. 17, the value of which is slightly lower than the value of AlN-2 in this work. The reason is that the thickness of AlN layer (245nm) used in Ref. 17 is lower than the one of AlN-2 (300nm), which confirms the accuracy of the fitting results in our work.



Downloaded from https://www.cambridge.org/core. Purdue University Libraries, on 03 Nov 2017 at 14:42:42, subject to the Cambridge Core terms of use, available at https://www.cambridge.org/core/terms. https://doi.org/10.1557/adv.2017.171

**Table.1** A list of samples and their SE fitting results.

| Sample name | Surface roughness (nm) | Thickness of HT-AlN layer (nm) | Bandgap at 300K (eV) |
|---|---|---|---|
| AlN-1 | 18.9 | 118 | 5.64 |
| AlN-2 | 3.5 | 300 | 6.06 |
| AlN-3 | 3.2 | 400 | 6.07 |

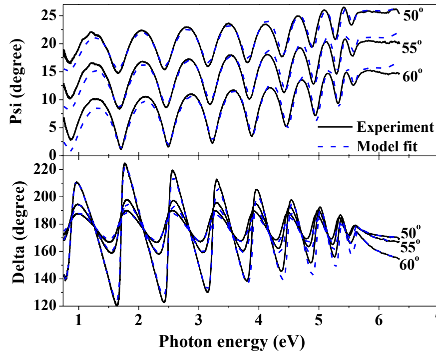


**Figure 1.** SE experimental and fitted psi and delta spectra vs. photon energy of incidence (50°, 55° and 60°) for AlN-3 sample at 825K.

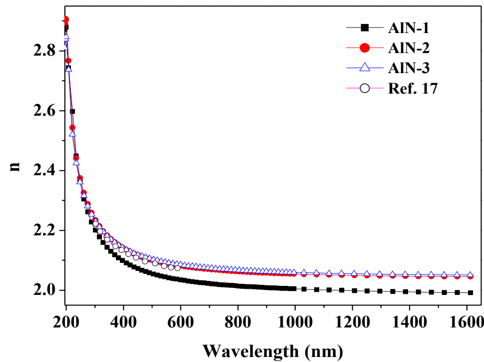


**Figure 2.** The fitted refractive indices vs. wavelength for three AlN samples at 300K.

Figure 3 shows the square of the absorption coefficient ($\alpha^2$) of three samples derived from SE fitting at 300K, and the energy bandgap can be estimated by using the linear fit of the well-known relation for direct band gap materials, Equation 1 [8]. The calculated bandgap of three samples are shown in Table 1, which indicates that the bandgap increases from 5.64 to 6.07eV as the thickness increases from 118 to 400nm. This could be attributed to the variable strain induced by point defects with different thickness of epi-layer [13].

$$(\alpha(\hbar\omega))^2 = A(\hbar\omega - E_g) \tag{1}$$



Downloaded from https://www.cambridge.org/core. Purdue University Libraries, on 03 Nov 2017 at 14:42:42, subject to the Cambridge Core terms of use, available at https://www.cambridge.org/core/terms. https://doi.org/10.1557/adv.2017.171

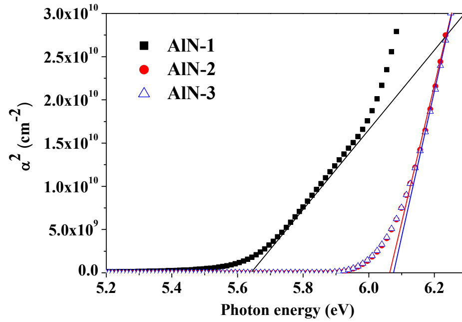


**Figure 3.** $\alpha^2$ vs. photon energy for three AlN samples at 300K.

Figure 4 shows the fitted refractive indices for AlN-2 and AlN-3 at 300, 475, 650 and 825K. It is observed that the refractive index increases in the transparent region as the temperature rises. The refractive index increases from 2.06 to 2.08 in the wavelength of 850nm as the temperature changes from 300 to 825K for the 404nm thick AlN epi-layer. Figure 5 gives the square of the absorption coefficient ($\alpha^2$) in the temperature range of 300K$\leq$T$\leq$825K for AlN-2 and AlN-3. The optical bandgap at elevated temperature can also be calculated from the linear fit, as shown in Figure 6. The absorption edge exhibits red-shift with the increase of temperature, which is correlated with the reduction of the bandgap. The decrease of bandgap with increasing temperature can be attributed to the effect of electron-phonon interactions and the lattice thermal expansion [8]. It is noted that, the absorption properties get worse as the temperature is higher than 475K, thus exhibiting a more pronounced reduction of bandgap. The phenomena can be attributed to the stronger electron-phonon interactions and the increased inter-atomic spacing induced by thermal expansion [18] at elevated temperatures.

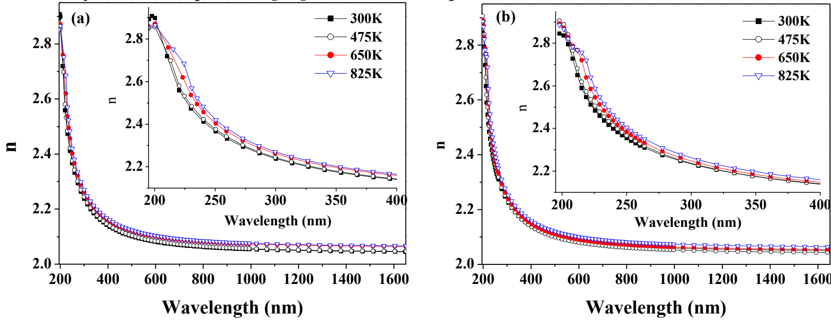


**Figure 4.** The fitted refractive index ($n$) at elevated temperature in the wavelength range of 195-1650nm for AlN-2 (a) and AlN-3 (b) samples. The inset shows the spectra in the wavelength range of 195-400 nm.

Figure 6 also shows the temperature dependence of $E_g$ derived from Ref.10 by PL measurements. The reported bandgaps lie slightly below the values in our work in the whole temperature range, which can be attributed to the non-interlayer inserted in the AlN structures of



Downloaded from https://www.cambridge.org/core. Purdue University Libraries, on 03 Nov 2017 at 14:42:42, subject to the Cambridge Core terms of use, available at https://www.cambridge.org/core/terms. https://doi.org/10.1557/adv.2017.171

Ref.10, and consequently increases the density of defects and dislocation in the epi-layer. The bandgap varies from 6.07 to 5.67eV for AlN-3 as the temperature rises from 300 to 825K, comparing with the reported variation of bandgap (from 6.0 to 5.54eV) with temperature (from 300 to 800K) for AlN thin film without AlN interlayer [10], which indicate that the thermal stability of bandgap on high temperature can be optimized by the inset of AlN interlayer in AlN thin films.

The decrease of bandgap is more pronounced in AlN-2 than that in AlN-3, indicating that the thermal stability of bandgap depends on the thickness of AlN epi-layer and the increasing thickness leads to a higher thermal stability of bandgap. The reason is that insufficient growth thickness of AlN epi-layer induces the incomplete coalescence of island in the growth process, which consequently result in poor surface morphologies and crystal qualities.

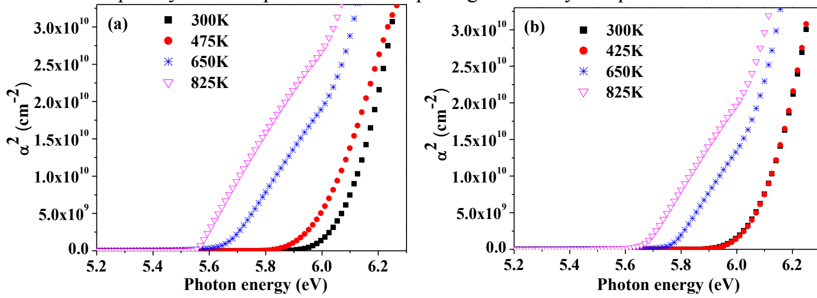


**Figure 5.** The square of the absorption coefficient ($\alpha^2$) vs. photon energy at elevated temperature for AlN-2 (a) and AlN-3 (b) samples.

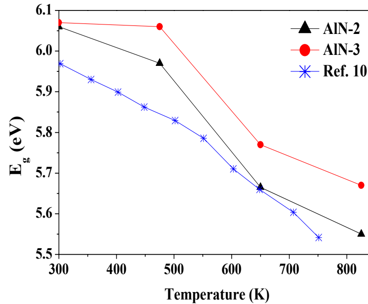


**Figure 6.** Temperature dependence of the bandgap values at 300-825K for AlN-2 and AlN-3 samples.

## CONCLUSIONS

In conclusion, the temperature-dependent (300-825K) optical properties of AlN thin films with different thickness of epitaxial layers are studied by spectroscopic ellipsometry. The results indicate that increasing the thickness of epi-layer leads to higher refractive index and higher bandgap. With the temperature increases, refractive indices almost increase in the transparent



Downloaded from https://www.cambridge.org/core. Purdue University Libraries, on 03 Nov 2017 at 14:42:42, subject to the Cambridge Core terms of use, available at https://www.cambridge.org/core/terms. https://doi.org/10.1557/adv.2017.171

region, while absorption properties degrade and bandgaps decrease. The reduction of band gap becomes more pronounced as the temperature is higher than 475K, and the thermal stability of bandgap becomes better by the insert of AlN interlayer and increasing the thickness of AlN epi-layer.

## ACKNOWLEDGMENTS

We acknowledge the funding support from US National Science Foundation (CMMI-1560834), National Natural Science Foundation of China (Grant Nos. 61367004 and 61504030), and Guangxi Science Foundation (Gant No. 2013GXNSFFA019001).

## REFERENCES

1. N. Lu and I. Ferguson, *Semiconductor Science and Technology* **28,** 074023 (2013).
2. P. Motamedi and K. Cadien, *Journal of Crystal Growth* **421**, 45-52 (2015).
3. K. Tsubouchi and N. Mikoshiba, *IEEE Trans. Sonics Ultrason.* **32**, 634-644 (1985).
4. M. Clement, L. Vergara, J. Sangrador, E. Iborra and A. Sanz-Hervás, *Ultrasonics* **42**, 403–407 (2004).
5. T. Aubert, O. Elmazria, B. Assouar, E. Blampain, A. Hamdan, D. Genève, and S. Weber, *IEEE Trans. Ultrason. Ferroelectr. Freq. Control* **59**, 999-1005 (2012).
6. T. Aubert, O. Elmazria, B. Assouar, L. Bouvot, and M. Oudich, *Appl. Phys. Lett.* **96**, 203503 (2010).
7. N. Watanabe, T. Kimoto, and J. Suda, *J. Appl. Phys.* **104**, 106101 (2008).
8. S. Sohal, W. Feng, M. Pandikunta, V. V. Kuryatkov, S. A. Nikishin, and M. Holtz, *Journal of Applied Physics* **113**, 043501 (2013).
9. H. He, L. Huang, Y. Zhang, Y. Fu, X. Shen, and J. Zeng, *Vacuum* **100**, 33-35 (2014).
10. K. B. Nam, J. Li, J. Y. Lin, and H. X. Jiang, *Appl. Phys. Lett.* **85**, 3489-3491 (2004).
11. H. Fujiwara, Spectroscopic Ellipsometry Principles and Applications, 1rd ed. (John Wiley & Sons, Ltd, England, (2007) p. 136.
12. M. Röppischer, R. Goldhahn, G. Rossbach, P. Schley, C. Cobet, N. Esser, T. Schupp, K. Lischka, and D. J. As, *J. Appl. Phys.* **106**, 076104 (2009).
13. M. Feneberg, M. Romero, B. Neuschl, K. Thonke, M. Röppischer, C. Cobet, N. Esser, M. Bickermann, and R. Goldhahn, *Thin Solid Films* **571**, 503–506 (2014).
14. G. Rossbach, M. Feneberg, M. Röppischer, C. Werner, N. Esser, C. Cobet, T. Meisch, K. Thonke, A. Dadgar, J. Bläsing, A. Krost, R. Goldhahn, *Phys. Rev. B* **83**, 195202 (2011).
15. S. Liu, X. Chen, C. Zhang, *Thin Solid Films* **584**, 176–185 (2015).
16. N.S. Das, P.K. Ghosh, M.K. Mitra, K.K. Chattopadhyay, *Phys. E Low-Dimens. Syst. Nanostruct.* **42**, 2097–2102 (2010).
17. N. Antoine-Vincent, F. Natali, M. Mihailovic, A. Vasson, J. Leymarie, P. Disseix, D. Byrne, F. Semond, J. Massies, *J. Appl. Phys.* **93**, 5222-5226 (2003).
18. Temperature dependence of the energy bandgap. Available at: http://ecee.colorado.edu/~bart/book/eband5.htm (accessed 23/10/2016).



Downloaded from https://www.cambridge.org/core. Purdue University Libraries, on 03 Nov 2017 at 14:42:42, subject to the Cambridge Core terms of use, available at https://www.cambridge.org/core/terms. https://doi.org/10.1557/adv.2017.171